Fast 2D-3D registration using GPU-based preprocessing

Kyehyun Kim[1], Sungjin Park[1], Helen Hong[2*], Yeong Gil Shin[1]

[1] School of Electrical Engineering and Computer Science, Seoul National University;
{iamkgh, sjpark, yshin}@cglab.snu.ac.kr
[2] School of Electrical Engineering and Computer Science, BK21: Information Technology,
Seoul National University, San 56-1 Shinlim 9-dong Kwanak-gu, Seoul 151-742 Korea
hlhong@cse.snu.ac.kr

Abstract—This paper describes the fast point-based 2-D/3-D registration that will increase the registration speed of intraoperative two-dimensional (2-D) fluoroscopy and preoperative three-dimensional (3-D) CT images using GPU (graphics processing unit)-based DRR's preprocessing. Rigid 2-D/3-D registration of 2-D fluoroscopy images with 3-D CT images can be used for image-guided surgery or intraoperative navigation. X-ray fluoroscopy images provide real-time visualization. However, in general, resolution of fluoroscopy images is limited, these modalities are only 2-D and features in the front of body overlap one. Because of its drawback, three-dimensional imaging modalities such as computed tomography (CT) and magnetic resonance (MR) imaging are broadly used in clinical diagnostics and treatment planning [1]. These have the spatial information and high resolution, but at present their use as interventional imaging modalities has been limited.

In this paper, to utilize CT information during interventional procedures, a preoperative CT scan is aligned with an intraoperative x-ray fluoroscopy image. In preprocessing procedure we generate CT-derived DRRs using graphic hardware. This method is over 150 times faster than software rendering. And for registration accuracy and speed, we propose point-based 2D-3Dregistration of phantom dataset. And to reduce computation cost, we apply point-based registration technique. Because this method leads the computation time to about one second, the registration speed is enough to apply to intervention.

1. INTRODUCTION

To develop image-guided surgery or intraoperative navigation system, 2-D/3-D registration of intraoperative 2-D imaging such as x-ray and preoperative 3-D imaging such as CT, MR is indispensable [2-5]. The key problem of 2-D/3-D registration is to compare input images that are of different dimensionalities. In order to estimate about relative spatial relationship of images, the images must be compared in the same space [1].

2-D/3-D registration technique is divided into two approaches. One approach is based on 3-D/3-D registration using 3-D reconstruction from 2-D images. The other approach is based on 2-D/2-D registration using 2-D Digitally Reconstructed Radiographs (DRR) generation from 3-D CT volume. For 2-D/3-D registration using 3-D reconstruction, closed-form solutions using quaternions and orthonormal matrices respectively of Horn [6] are generally used. This technique requires several 2-D images. However, real-time obtainment of 2-D images is not easy during operation.

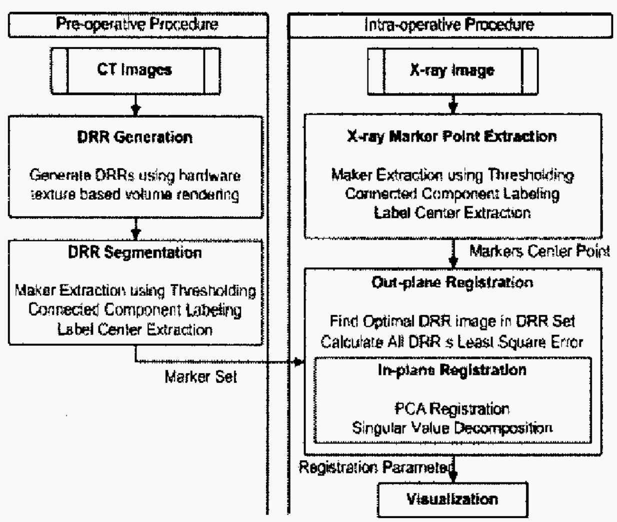

Figure 1. The flowchart of 2-D/3-D registration

2D-3D registration using 2-D DRR generation requires thousands ray-casting steps. It is heavy task. For registration of

* Corresponding author.

skull, pelvis, and spine, Zollei [1] used mutual information registration technique. And for registration of vertebra, Weese [7] used DRR generation of small sectional CT and pattern intensity registration technique. Because these techniques require thousands of computation time, real-time application is imposible.

In real-time to visualize anatomical information in 2-D x-ray image, this paper proposes a fast registration method of the 2-D images from 3-D volume using GPU-based DRR's preprocessing. For this registration task, our method is composed of three main steps: fast CT-derived DRR generation using graphic hardware, automatic extraction of marker using connected component algorithm and point-based 2-D/3-D registration using in- and out-plane registration (see figure 1).

2. FAST DRRS GENERATION

Simulated projection images from CT volume are called Digitally Reconstructed Radiographs (DRRs) [7]. In general, these images are computed with the so-called ray-casting algorithm from a CT volume of the patient acquired before surgical operation. Ray-casting algorithm is to compute an amount of light that a virtual ray from X-ray light source penetrates 3D CT, and it arrives image surface like figure 2. As this algorithm must visit every voxel of CT volume while computing the projection image, it is needed to much computational time. In order to reduce the computational time, early ray termination is generally used. However, early ray termination is not able to apply our method because we do not use opacity transfer function and we apply Maximum Intensity Projection (MIP) to our composing method. Thus, one DRR slice generation takes about 100seconds on Intel Pentium 4 CPU 2.4Ghz machine. Besides, a few thousand of DRRs are required for 2-D/3-D registration. In order to overcome the very heavy task of DRRs generation, this paper proposes a GPU-based DRRs generation using graphics hardware.

The DRRs image is generated by texture-based volume rendering method using high level shading language (HLSL). At first, we generate three dimensional volume data using acquired each CT slice images like figure 3. When acquired CT slice images, we are able to know about an interval of each slice images. We generate three dimensional volume data by interpolating the interval using nearest neighbor interpolation.

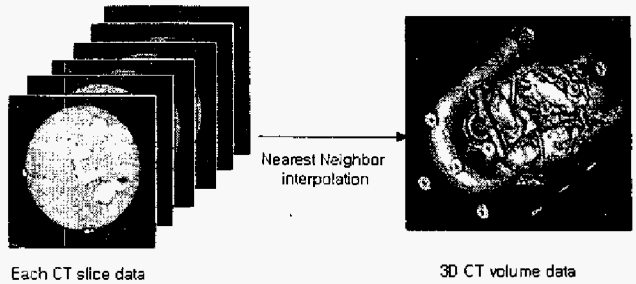

Figure 3. A generation of three dimensional volume data

When loading a volume data in three-dimensional texture, it is impossible to load the data if a resolution of the data is over 512x512x512. Thus, we alter the volume data size of each voxel from 12bit to 8bit, and we load the 8bit volumetric data in three-dimensional texture. Although the method may happen to lose information, it is not serious problem. Our objective is to segment the markers and perform registration between DRRs and X-ray image. Moreover, the markers have a high intensity value, so it is possible to take a higher 8 bit data from 12 bit data to segment markers.

After loading in the texture, we apply texture-based volume rendering method. In general, proxy geometry is generated using parallel projection. As simulating X-ray image, we generate proxy geometry using perspective projection. Figure 4 shows a proxy geometry generation method.

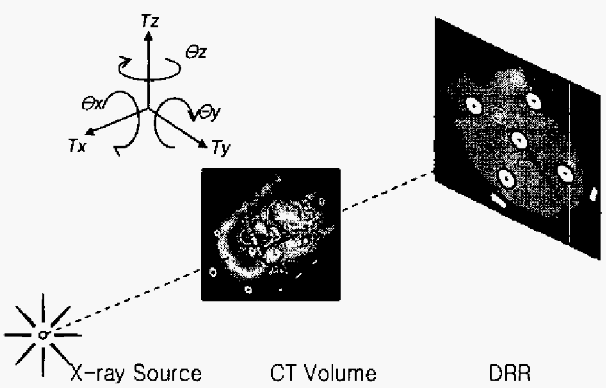

Figure 2. DRRs generation using CT volume data

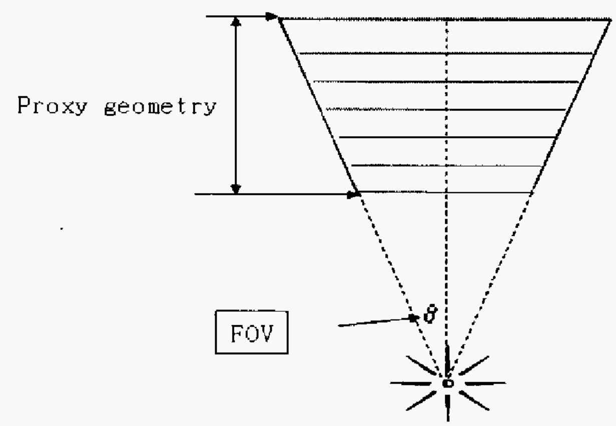

Figure 4. A generation of proxy geometry using perspective projection

We map three-dimensional texture in the memory of graphics hardware onto generated proxy geometry. The mapped slices onto proxy geometry render using a compositing mode. The compositing mode consists of three techniques: minimum intensity projection, average intensity projection, and maximum intensity projection. Among them, we select maximum intensity projection that is the best method to represent the markers.

The DRRs image quality acquired from this method is as good as the image quality acquired from ray casting method as shown in Figure 5. Moreover, one DRRs slice generation from this method takes about 0.45 seconds on Intel Pentium 4 CPU 2.4GHz machine and ATI Radeon 9600 GPU with 256MB of memory.

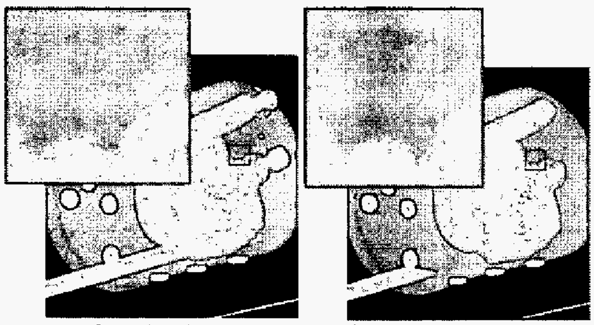

(a) software-based DRRs (b) hardware-based DRRs

Figure 5. Result Images of SW/HW Rendering

3. Automatic Markers Segmentation

For point-based registration, automatic confirmable markers segmentation method is used. However, x-ray images lack clearness, have low sensitivity, and have noises. In order to accurately extract, we automatically extract markers using thresholding [8] and connected component method. First, candidate regions of markers from each x-ray images, we use housefield unit value above a chosen threshold. And then these regions saved as binary maps. Second, because there are noise and other features in these maps, they must be removed. They are identified using connected component algorithm. Identified regions are compared with standard marker model. If they are small or large than standard marker model, they are regarded as noises or other features. Finally, centroids of extracted regions are computed.

Figure 6 shows result of 2-D/3-D registration. The red region is markers of x-ray, and the cross markers are centroids of marker of CT.

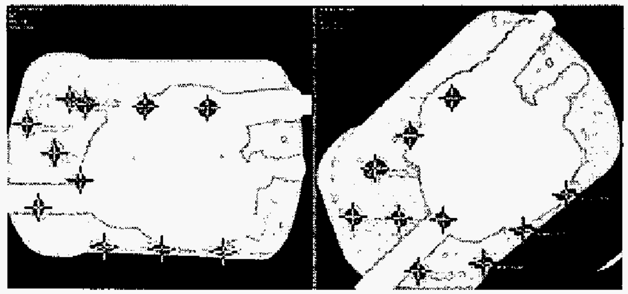

Figure 6. The Segmentation Results

4. Registration

2-D/3-D registration is to align the coordinate of 2-D x-ray image with the coordinate of 3-D CT or to determine the correspondence between the intraoperative x-ray image and the preoperative CT volume. In order to determine the transformation in three-dimension space, in general, translation and rotation components for x, y, and z axis are computed in six degrees-of-freedom. But this system increases computation cost in six degrees. In this paper, to reduce the growth rate of computation cost, we propose separated registration steps of out-plane registration and in-plane registration. This method leads the computation cost to just two degrees.

Out-plane registration is to compute the position of x- ray source in 3-D space. To find the source position, we apply to two rotation vectors of spherical coordinate system and search the rotation vectors that optimize the correspondence between x-ray image and CT volume. In order to estimate the similarity, we use the root-mean-square-error (RMSE) of the in-plane registration result. RMSE defined by

$$RMSE = \sqrt{\frac{1}{n}\sum_{i=1}^{n}\left\|P_{ij} - T_i\right\|^2}$$

where T_i is x-ray marker and P_{ij} is nearest CT marker with T_i.

In 2-D in-plane registration step, we determine the optimal translation and rotation vectors of markers using the principle axes registration method [9,10]. This method computes each axes of markers in two images using the Singular Value Decomposition (SVD) as

$$A = U\Sigma V^T \quad \Leftrightarrow \quad \Sigma = U^T AV \qquad (1)$$
$$\Sigma = diag(\sigma_1, \cdots, \sigma_r)$$

where U and V are unitary, and Σ is real diagonal elements. The σ_i are called the singular values. In-plane rotation vector θ is the differential angle between axes. And in-plane translation vectors T_X, T_Y for each axis is computed by the weighted mean of the markers' center positions.

TABLE I
EXPERIMENTAL DATASETS

Experimental Dataset	CT Set	Image Resolution	CT Slice Number	DRR Interval	DRR Slice Number
Data A	CT 1	512*512	566	0.5	3600
Data B	CT 2	512*512	391	0.5	3600
Data C	CT 1	512*512	566	1	900
Data D	CT 2	512*512	391	1	900
Data E	CT 1	512*512	566	2	225
Data F	CT 2	512*512	391	2	225

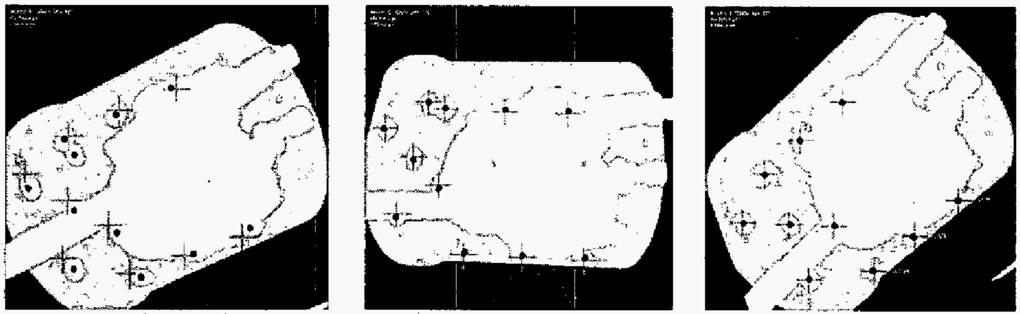

(a) Registration of 2 degree interval DRR (b) Registration of 1 degree interval DRR (c) Registration of 0.5 degree interval DRR

Figure 7. 2-D/3-D Registration Results

5. RESULTS

All our implementation and test were performed on an Intel Pentium IV PC containing 2.4 GHz CPU and 1.0 GBytes of main memory. Our method has been successfully applied to two phantom datasets for evaluating accuracy and computation time. Dataset A and B have 3600 DRRs with intervals of 0.5 degree, dataset C and D have 900 DRRs with intervals of 1 degree, and dataset E and F have 225 DRRs with interval of 2 degree (see table I).

Table II shows DRR generation time using graphic hardware (HW) and software (SW) rendering techniques. HW rendering technique is over 150 times faster than SW rendering technique.

TABLE II
DRR GENERATION TIME OF HW/SW

Experimental Dataset	HW rendering (min)	SW rendering (min)
Data A	24.21	5707.85
Data B	23.48	3664.28
Data C	6.02	1427.01
Data D	5.87	916.06
Data E	1.50	356.67
Data F	1.47	229.03

Table III shows that the registration speed is enough to apply to intervention. The computation time was less than 0.05 seconds in dataset A and 0.1 seconds in dataset B. And registration time increases in proportion to the number of DRRs.

TABLE III
PROGRESSING TIME OF 2-D/3-D REGISTRATION

Experimental Dataset	Processing Time (millisec)
Data A	1372
Data B	1286
Data C	315
Data D	369
Data E	87
Data F	92

In figure 7, background images are x-ray images, black points express markers of x-ray images, and crisscross patterns express markers of CT. In case of registration of 2 degree interval DRR, markers of CT are not matched with markers of x-ray. The other sides, in case of registration of 1 or 0.5 degree interval DRR, markers are exactly matched.

For accuracy test, we evaluated the root-mean-square-error (RMSE) between DRRs and x-ray markers. In our experiments, RMSE is less than 3 in dataset A and 20 in dataset B. Experimental results showed that our method is as accurate as

TABLE II
EVALUATING ACCURACY OF 2-D/3-D REGISTRATION

Dataset	Translation Parameter		Rotation Parameter			RMSE
	Ground-Truth Parameter		Ground-Truth Parameter			
	(Tx, mm)	(Ty, mm)	(θx ,deg)	(θy ,deg)	(θz ,deg)	
Data A	30.9	30.1	53.5	48	56.5	2.7
	31	29	53.7	47.9	56.3	
Data B	12.3	17.6	35.5	50.5	45.5	1.8
	12	18	35.7	50.3	45.4	
Data C	29.7	46.4	32	50	42	11.3
	29	47	31.6	50.5	41.6	
Data D	22.5	30.8	36	42	42	8.6
	24	30	36.2	41.6	41.9	
Data E	20.6	28.8	54	54	48	19.7
	21	27	54.9	53.5	49.4	
Data F	15.7	15.8	47	36	54	22.7
	16	15	46.1	36.9	54.8	

the conventional registration and gives more fast computation than the conventional one.

CONCLUSION:

We proposed the fast point-based 2-D/3-D registration using GPU-based DRRs generation and in-/out-plane registration for multi-dimensional registration. Our GPU-based DRRs generation algorithm was performed rapidly. The proposed marker extraction could remove the noise with accuracy using the connected component-based labeling. The in- and out-plane registration reduces the search space to two degrees-of-freedom from six degrees-of-freedom. And processing time is sufficient to apply to real-time surgery such as image-guided surgery or intraoperative navigation.

REFERENCE

[1] Zöllei, E. Grimson, A. Norbash, W. Wells: "2D-3D Rigid Registration of X-Ray Fluoroscopy and CT Images Using Mutual Information and Sparsely Sampled Histogram Estimators", IEEE CVPR, 2001.

[2] Gage BF, Waterman AD, Shannon W, Boechler M, Rich MW, Radford MJ. Validation of clinical classification schemes for predicting stroke: results from the National Registry of Atrial Fibrillation. Jama 2001; 285:2864-70.

[3] Cox JL, Schuessler RB, D'Agostino HJ, Jr., et al. The surgical treatment of atrial fibrillation. III. Development of a definitive surgical procedure. J Thorac Cardiovasc Surg 1991; 101:569-83.

[4] Wyse DG, Waldo AL, DiMarco JP, et al. A comparison of rate control and rhythm control in patients with atrial fibrillation. N Engl J Med 2002; 347:1825-33.

[5] Swartz J, Perrersels G, Silvers J, Patten L, Cervantez D. A catheter based curative approach to atrial fibrillation in humans (abstract). Circulation 1994.

[6] Berthold K. P. Horn. Closed-form solution of absolute orientation using unit quaternions. Journal of the Optical Society of America A, 4(4):629–642, April 1987.

[7] J. Weese, R. Goeke, G.P. Penney, P. Desmedt, T.M. Buzug, H. Schumann "Fast voxel-based 2D/3D registration algorithm using a volume rendering method based on the shear-warp factorization" Medical Imaging 1999: Image Processing; Proceedings of SPIE Vol 3661, 1999, p 802-810.

[8] R.G Gonzalez, R.E. Woods, "Digital Image Processing," Addison Welsey, pp.443-458, Sep. 1993

[9] Rusinek, H., Tsui, W., Levy, A. V., Noz, M. E. and de Leon, M. J. (1993) Principal axes and surface fitting methods for threedimensional image registration. J. Nucl. Med., 34, 2019–2024.

[10] Alpert, N. M., Bradshaw, J. F., Kennedy, D. and Correia, J. A. (1990) The principal axis transformation––a method for image registration. J. Nucl. Med., 31, 1717–1722.